

## **General Disclaimer**

### **One or more of the Following Statements may affect this Document**

- This document has been reproduced from the best copy furnished by the organizational source. It is being released in the interest of making available as much information as possible.
- This document may contain data, which exceeds the sheet parameters. It was furnished in this condition by the organizational source and is the best copy available.
- This document may contain tone-on-tone or color graphs, charts and/or pictures, which have been reproduced in black and white.
- This document is paginated as submitted by the original source.
- Portions of this document are not fully legible due to the historical nature of some of the material. However, it is the best reproduction available from the original submission.

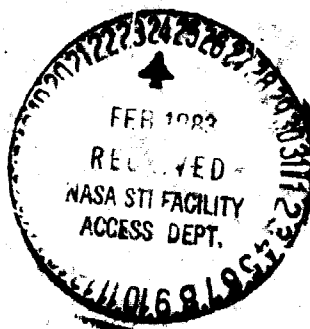
# Aircraft Typhoon Mise

(NASA-TM-83317) AIRCRAFT TURECFAN NCISE  
(NASA) 17 P HC A02/MF A01 CSCL 20A

N83-18405

Unclassified  
G3/71 02817

John P. Groeneweg and Edward C. Rice  
*Lewis Research Center*  
*Cleveland, Ohio*



**Prepared for the  
Twenty-eighth Annual International Gas Turbine Conference  
sponsored by the American Society of Mechanical Engineers  
Phoenix, Arizona, March 27-31, 1983**

**NASA**

**ORIGINAL PAGE IS  
OF POOR QUALITY**

## AIRCRAFT TURBOFAN NOISE

John F. Groeneweg and Edward J. Rice  
National Aeronautics and Space Administration  
Lewis Research Center  
Cleveland, Ohio 44135

### ABSTRACT

Recent advances in the understanding of turbofan noise generation and suppression in aircraft engines are reviewed with particular emphasis on NASA research. The review addresses each link in the chain of physical processes which connect unsteady flow interactions with fan blades to far field noise. Mechanism identification and description, duct propagation, radiation and acoustic suppression are discussed. Recent advances in the experimental technique of fan inflow control assure that in-flight generation mechanisms are not masked by extraneous sources in static tests. Rotor blade surface pressure and wake velocity measurements aid the determination of the types and strengths of the generation mechanisms. Approaches to predicting or measuring acoustic mode content, optimizing treatment impedance to maximize attenuation, translating impedance into porous wall structure and interpreting far field directivity patterns are illustrated by comparisons of analytical and experimental results. A persistent theme of the review is the interdependence of source and acoustic treatment design to minimize far field noise. Areas requiring further research are discussed and the relevance of aircraft turbofan results to quieting other turbomachinery installations is addressed.

### INTRODUCTION

Over the past decade the noise generated by the fan component of aircraft turbofan engines has been the subject of vigorous research. The emphasis on the fan reflects the fact that, for the high bypass engines which dominate the world fleet of large commercial transports, the fan controls flyover noise on landing approach and is a strong contributor along with jet noise on takeoff. Indeed, for the next generation of turbofan engines the prominent contribution of the fan to propulsion system noise is projected to continue. Figure 1 shows the results of a system noise prediction done as part of an energy efficient engine design study (1). Component noise levels in terms of tone corrected perceived noise decibels are given at take-

off and approach conditions. The fan controls the totals at both conditions even with the suppression provided by substantial use of acoustic treatment. Similar conclusions about the importance of fan noise have been drawn in other studies (2,3). The purpose of this paper is to review recent results of research on fan noise generation and suppression, and to identify significant gains and remaining gaps in our understanding and ability to predict and control this annoying source.

The scope of this review is limited to results drawn mainly from NASA initiated work carried out in roughly the last five years. We believe that this definition of scope, relaxed and supplemented in specific areas, leads to a reasonably accurate picture of the state-of-the-art while not attempting to exhaustively cover parallel efforts and results. Several existing reviews provide extensive bibliographies and summarize earlier results in turbomachinery noise (4), flight effects (5), and suppressors (6,7). Our review builds upon, but, primarily, extends and updates these earlier efforts to cover significant advances in experimental flight simulation techniques, diagnostic measurements, theoretical modelling and computation.

The flow chart in Fig. 2 illustrates the chain of physical processes which links unsteady aerodynamics of the fan flow field to the resultant far field acoustic signature. Elements in ovals are inputs to, or outputs of, the processes in the rectangles. The four processes--(i) blade unsteady aerodynamic response, (ii) coupling to the duct, (iii) propagation in the duct which may have acoustically treated walls, and (iv) acoustic coupling (radiation) to the far field--have each been studied and modelled separately as convenient subdivisions of the overall problem. A knowledge of the inputs and outputs--(i) unsteady flow field disturbances, (ii) blade surface pressure distributions, (iii) duct acoustic mode content at the entrance, and (iv) exit of the duct--is required to link the processes and arrive at the final output which is far field directivity (and spectra). Of course, from an experimental viewpoint, the intermediate inputs or outputs are often missing; only acoustic measurements in the far field are available.

## ORIGINAL PAGE IS OF POOR QUALITY

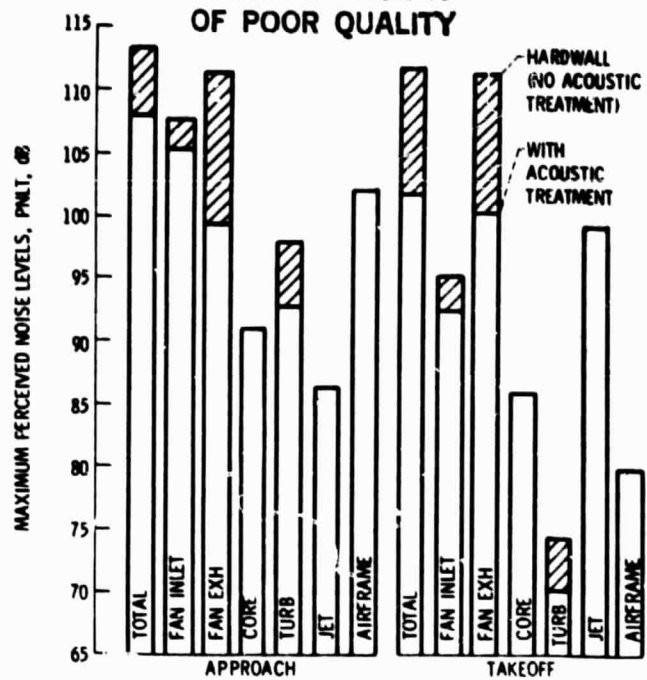


Figure 1. - Flyover component noise levels for an advanced turbofan.  
(Ref. 1)

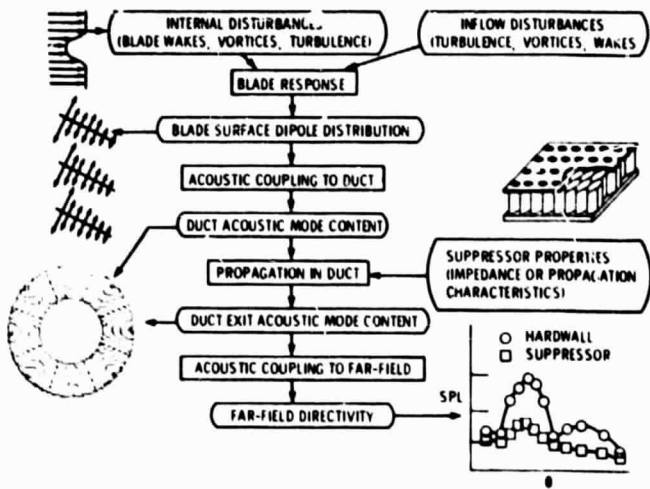


Figure 2. - Elements of fan noise generation and suppression.

In fact, one of the greatest hindrances to applying the theories for the individual processes to practical situations has been the lack of definition of the key input/output quantities at the interfaces. Recent diagnostic measurements and analyses have begun to correct this deficiency. This review is organized around the elements of Fig. 2.

### GENERATION PROCESSES

#### Mechanism Identification

The primary input to the fan noise generation process at subsonic tip speeds is a description of the unsteady aerodynamic fluctuations encountered by a blade row. In spectral terms, random fluctuations produce broadband or narrowband (tone-like) random noise while periodic fluctuations produce tones at

multiples of the blade passing frequency. At supersonic tip speeds the added phenomenon of multiple pure tones associated with rotor-locked leading edge shocks comes into play at multiples of shaft rotation frequency. The initial task of fan noise description is to identify the dominant mechanisms in terms of the origin of the responsible flow disturbance and the blade row with which it interacts. On the engine cross section in Fig. 3, some of the candidate turbofan mechanisms are labeled with flow disturbances grouped according to the blade row with which they interact. Sample narrowband spectra which identify the components associated with subsonic and supersonic tip speeds are also shown. Most progress has been made in understanding the generation of tones which usually dominate the spectrum levels; the relative importance of potential broadband generation mechanisms such as those associated with inlet boundary layer or wake turbulence remains vague.

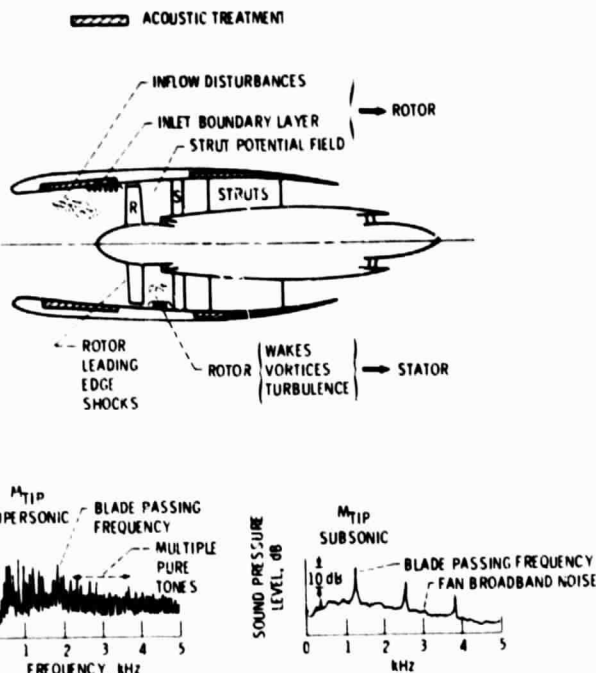


Figure 3. - Turbofan noise generation mechanisms and spectra.

Flow disturbances are divided into two categories in Fig. 2: those originating external to the engine but drawn into the inlet, and those originating inside the engine. While it has long been recognized that ingested external disturbances may control fan noise generation (8); it was the high bypass engine flyover noise data, acquired in connection with noise certification requirements, which established that ground test tone levels were controlled by extraneous inflow disturbances unrepresentative of flight (5). In fact, the practicality of the concept of choosing vane-blade ratio for cutoff (9,10) to greatly reduce the fundamental tone was, at first, only confirmed in flight or in a wind tunnel as shown by the examples in Fig. 4.

**Flight Simulation.** The approach to controlling the inflow for flight simulation in static tests has evolved around the concept of inlet honeycomb-grid flow conditioners which must be acoustically transparent over the frequency range of interest. Figure 4 shows the range of inflow control devices (ICD's) investigated at NASA Lewis (11, 12, 13, 14). The sizes of the external devices, Figs. 5(a) and (b)

ORIGINAL PAGE IS  
OF POOR QUALITY

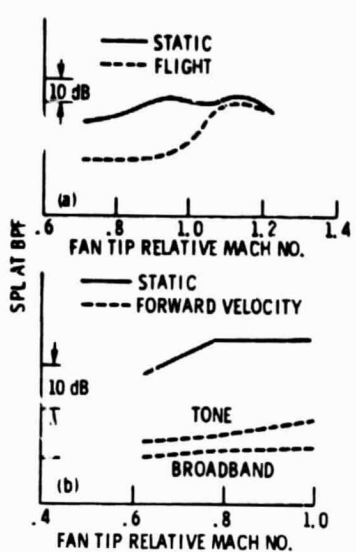


Figure 4. - Effect of forward velocity on the fan blade passing tone in the inlet duct. (Ref. 5.)

ranged from roughly 4 to 2 fan diameters. An induct honeycomb, Fig. 5(c), was found to be aerodynamically effective but unacceptable from an acoustic transmission standpoint. The first generation design, Fig. 5(a), drew on flow conditioning work for turbulence reduction (15) to arrive at the screen-honeycomb composite structure. The most recent

version, Fig. 5(b), is reduced in size, uses honeycomb only, and employs thinner support ribs with more carefully bonded joints and cleaner attachment to the inlet lip. The shape conforms to an equipotential surface.

Acoustic results for a JT15D engine in terms of fundamental blade passing tone and broadband directivities are shown in Fig. 6 for the two ICD's. Residual tone levels with inflow control approach the broadband over much of the angle range at these low fan speeds. Interestingly, the broadband levels remain essentially unchanged with inflow control indicating that another mechanism, probably internal to the fan, controls this spectral component.

Flight data from the JT15D on an OV-1 test-bed aircraft (14) confirm the effectiveness of the ICD of Fig. 5(b) as shown in Fig. 7. The fundamental tone directivity with inflow control agrees well with the flight data except at the most forward angles where signal-to-noise ratio is low for flight.

Blade surface pressure measurements have proved to be a valuable diagnostic tool in evaluating the quality of inflow to the fan and, with inflow control, in determining the residual internal sources controlling flight levels. Miniature pressure transducers mounted near the fan blade leading and trailing edges at several spanwise locations are used in conjunction with a telemetry system (8,12,16) to continuously survey the circumferential variation of unsteady blade pressures. This technique originally identified longitudinally persistent, circumferentially localized disturbances attributed to atmospheric turbulence elongated by the streamtube contraction in the inflow (8). Such disturbances, which may also be caused by ingested vortices, wakes and instabilities associated with flow around the inlet lip, produce strong narrow-band random tones.

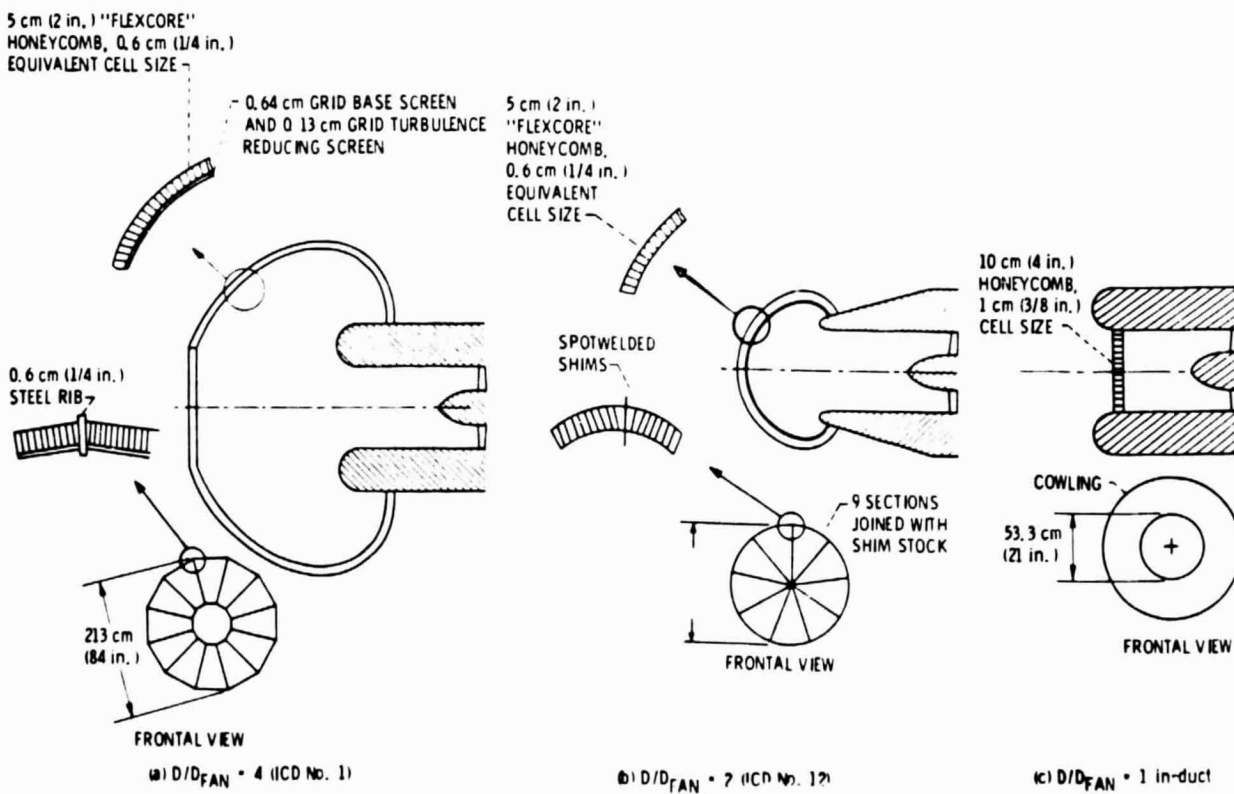


Figure 5. - Inflow control devices for flight fan noise simulation tested at Lewis Research Center. (Ref. 12)

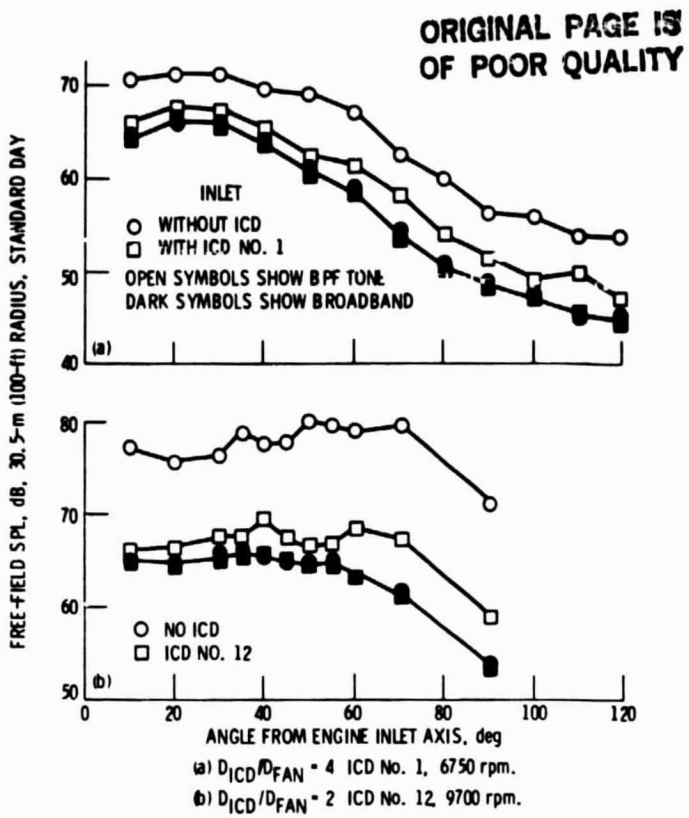


Figure 6. - Far field directivity with inflow control devices in JT150 engine,  $\Delta f = 25$  Hz. (Ref. 12)

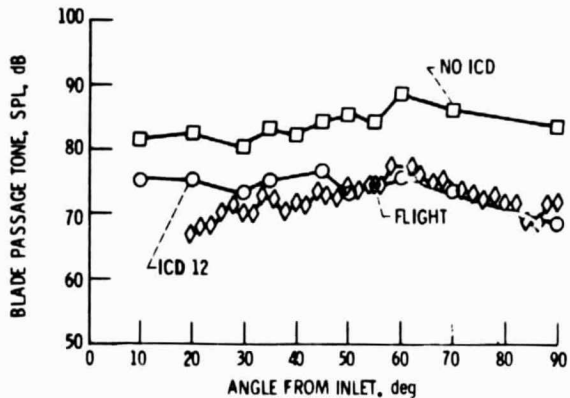


Figure 7. - Effectiveness of inflow control for flight fan tone simulation. (Ref. 14)

Figure 8 compares narrowband blade pressure spectra without and with inflow control. Without an ICD, Fig. 8(a), the spectrum shows strong harmonic content at all multiples of shaft rotation frequency resulting from multiple encounters of the blade transducer with circumferentially varying flow disturbances. The additional scales on the abscissa are distortion number (multiple of shaft frequency) and the circumferential acoustic mode number corresponding to blade number minus distortion number. Inflow control eliminates the randomly varying disturbances and the corresponding bulk of the shaft harmonics as illustrated in Fig. 8(b). Those distortion numbers that remain are associated with periodic, internally generated flow disturbances which are fixed in space or have fixed rotation rates with respect to the rotor. As a result, clues to the mechanisms governing flight levels are found from the prominent residual peaks.

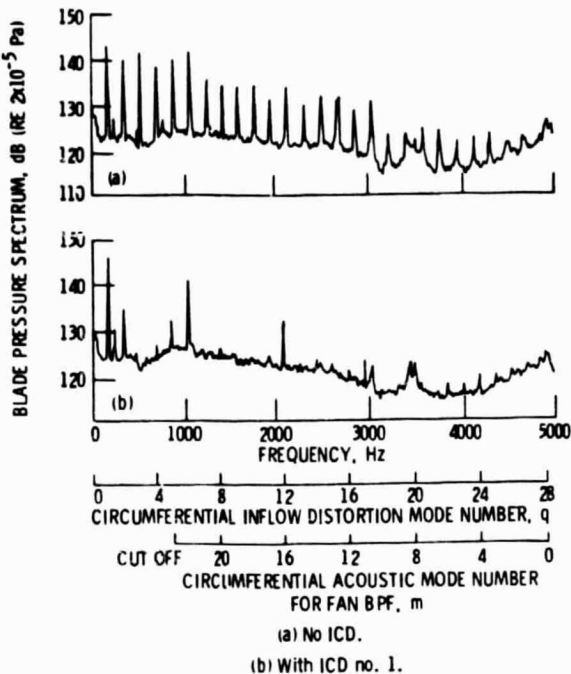


Figure 8. - Narrowband blade pressure spectra, pressure side transducer 1.9 cm from tip, JT150 engine, 10500 rpm. (Ref. 12)

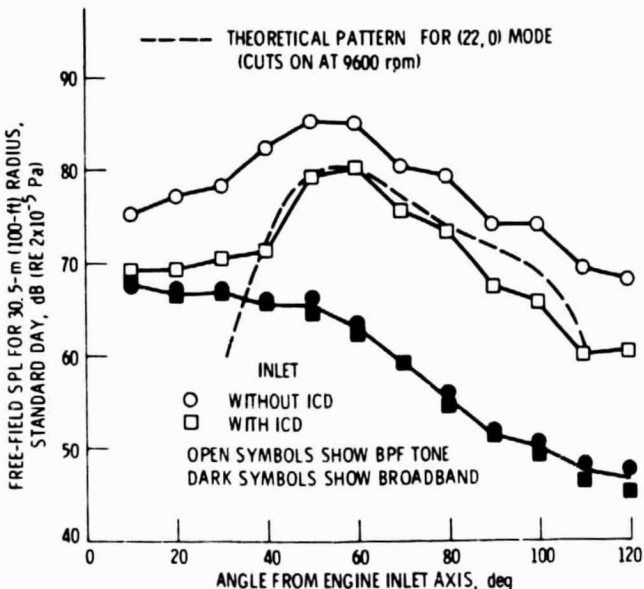


Figure 9. - Directivity pattern indicating presence of 22-lobed circumferential mode due to rotor-strut interaction, JT150 fan, 10500 rpm. (Ref. 12)

Substantial effort has also been applied to the inflow control problem by industry (16-23) including flyover level comparisons to static projections (22) and development of ICD design procedures (23). The first generation of large engine ICD's, roughly 3 fan diameters in size, is currently in use. Although the quantitative agreement of inflow control and flight data is still subject to some improvement, the current "state-of-the-art" does allow the study of bona fide internal sources controlling fan noise generation in flight. An alternative to ICD's are anechoic wind tunnels (24-26) which also have been found to eliminate

# ORIGINAL PAGE IS OF POOR QUALITY

the bulk of the extraneous inlet disturbances

In-Flight Sources. Once the study of internal mechanisms is made possible by inflow control, the task becomes one of identifying the interactions responsible for the tone levels observed over the range of engine speeds. Rotor wake-stator interaction remains a prime mechanism; but, even with the blade-vane ratio chosen to prevent fundamental tone propagation, other interactions may come into play. For example, the JT15D engine exhibits a strong fan fundamental tone which appears at a speed corresponding to the start of propagation of the 22-lobed acoustic mode as shown in Fig. 9(12). The source of the 22-lobed acoustic mode is the interaction between the 28 fan blades and the six structural support struts downstream of the fan stator. The blade pressure spectrum in Fig. 8(b) shows that a strong 6-per revolution disturbance is sensed on the rotor. A prime candidate for the interaction mechanism is a strut potential field extending upstream through the stators and interacting with the rotor. An alternate explanation would be the interaction of residual rotor wakes with the six engine struts generating the 22-lobed spinning acoustic mode which is sensed on the rotor as a 6-per revolution disturbance. Existing large high-bypass turbofans also contain downstream struts. The next generation of engines will incorporate integral strut-stator vane assemblies with a potential for still more complicated interactions (27).

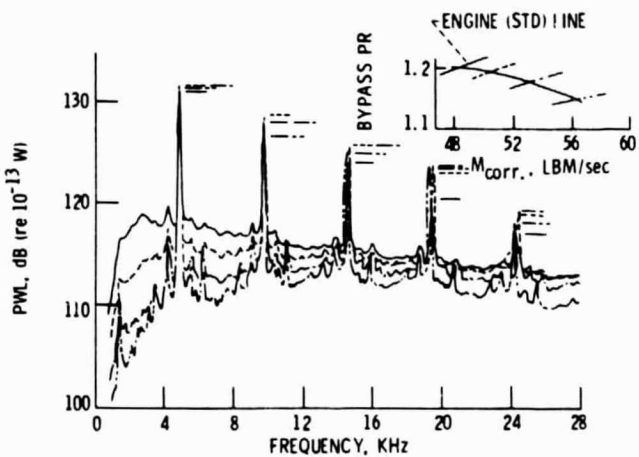


Figure 10. - Variation of broadband levels with fan operating point, JT15D fan in anechoic chamber  $\Delta f = 80$  Hz, 10500 rpm.

As mentioned earlier, the random disturbances responsible for broadband generation appear to be internal. Broadband levels vary strongly with fan operating point (rotor incidence angle or loading) as shown in Fig. 10. Fan blade suction surface flow separation and interaction with the trailing edge, blade tip interaction with the casing boundary layer and rotor wake turbulence (midspan or tip) interaction with the stator are candidate mechanisms although the latter seems to be discounted by rotor alone experiments (28).

While the multiple pure tone (MPT) generation mechanism is clearly associated with the rotor leading edge shocks and their blade-to-blade nonuniformity, quantitative descriptions of the source are lacking. Two aspects of the process have been investigated in connection with concepts to reduce this strong inlet source at takeoff fan speeds. First, a radical fan with compound leading edge sweep was designed to keep the normal component of blade inlet relative Mach num-

ber subsonic over the entire span (30). Except for blade end effects and the sweep reversal point, a major portion of the strong leading edge shock system was expected to be eliminated. Figure 11 shows the measured MPT power results obtained with the swept design compared to a conventional, unswept fan (31). Sweep delayed the onset of MPT's and reduced the levels over a large portion of the tip-speed range including takeoff. The second aspect of inlet noise generation at supersonic tip speeds concerned the observation that total tone power peaks beyond the transonic speed and then falls off. A fan designed for unusually high specific flow,  $220 \text{ kp/sec.m}^2$ , at high tip speed,  $553 \text{ m/sec}$ , exhibited a marked tone power decrease at design (32) although not qualitatively different from other high tip speed designs. The phenomenon appears to be only partially attributable to propagation inhibiting effects of elevated inlet Mach numbers and may be associated with non-linear propagation characteristics in combination with the angle and associated strength variations of the leading edge shocks (33).

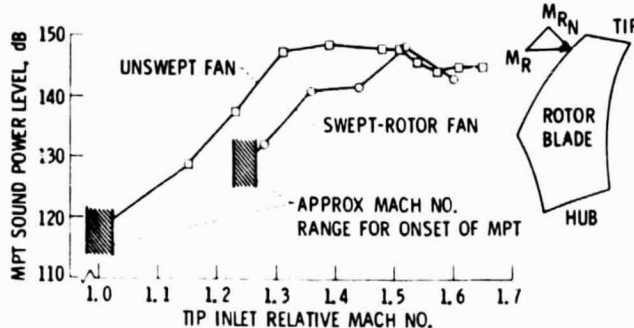


Figure 11. - Effect of rotor leading edge sweep on multiple pure tone generation. (Ref. 31)

## Mechanism Description

Ducted Cascade Response. Considerable effort has been expended within the last five years to model the noncompact compressible response of a ducted cascade of blades to unsteady upwash velocities. Perhaps the most complete description available is the three-dimensional lifting surface theory (34) for a rotating cascade in an annular duct. This blade response and duct coupling analysis is the heart of specialized studies of rotor-inflow distortion (35) and rotor-stator interaction (36). These linear analyses are for the dipole-type sources at the surface of a cascade of thin (in some cases twisted) blades and represent exact solutions to the linearized continuity and momentum equations (37, Chap. 5).

Three features of these analyses are considered to be important advances. First, the 3D approach makes possible the calculation of the circumferential and radial content of acoustic modes in annular or cylindrical ducts; the complete description of modal content is precisely the input required for successive propagation analyses. Second, cascade analysis predicts chordwise unsteady pressure distributions and integrated responses which differ substantially from single blade results (38,39) that ignore blade-to-blade interactions (solidity) and the interblade phase angle of the disturbance. Third, source non-compactness, retained by calculating chordwise in addition to spanwise pressure fluctuations, has been shown to produce significant differences in calculated power compared to compact analyses. The magnitudes of the differences, which depend on incident disturbance shape and

propagation direction with respect to the mean flow, are highest for single distortion modes (38). For realistic distortion profiles represented by a combination of distortion modes, the effects of noncompactness are less dramatic with a tendency for the compact analysis to underestimate fundamental tone power for upstream propagation and overestimate the power propagating downstream(35).

Since full 3D calculations are complex and lengthy, a quasi-3D analysis, which uses 2-D (strip) theory for aerodynamic response but annular duct acoustics for modal prediction, was investigated (35). The results indicated that the quasi-3D approach produced relatively small errors in power, greatly reduced computation time, and fulfilled the requirement to predict annular duct acoustic modes. Consequently, the quasi-3D approach was adopted in the development of a computer program (40) which considered three types of flow disturbances: inlet turbulence, rotor mean wakes and rotor wake turbulence. This quasi-3D approach is still being evaluated by data-theory comparisons.

The 3-D lifting surface tone power predictions have been compared to fan noise data (41) where the controlled source consisted of the fan interacting with an array of inlet distortion rod wakes. Figure 12 shows excellent agreement between the predicted total inlet fundamental tone power as a function of fan speed and the measured narrowband tone power obtained from far-field measurements. Note the changing mix of radial mode contributions to the totals and the non-monotonic increase with speed in both theory and data.

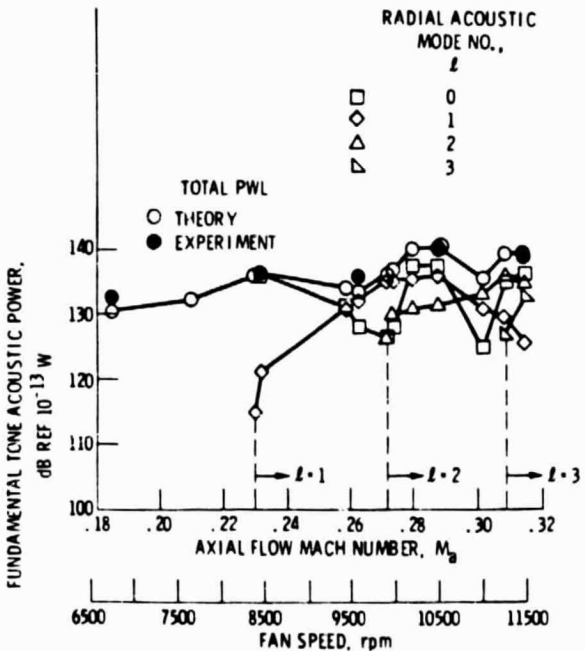


Figure 12. - Speed dependence of inlet fundamental tone modal power generated by 41 rod wakes interacting with a JT15D fan. (Ref. 41)

The intermediate quantity between blade response and duct coupling is blade pressure (Fig. 2). The cascade response portion of the code in (40), was used to calculate the chordwise magnitude of the unsteady blade pressures due to interaction with Gaussian wakes produced by upstream radial rods. As shown in Fig. 13, the high disturbance frequency associated with many (41) rod wakes is predicted to produce many rapid changes in pressure along the chord. Typical miniature transducer sizes are indicated near the leading and

## ORIGINAL PAGE IS OF POOR QUALITY

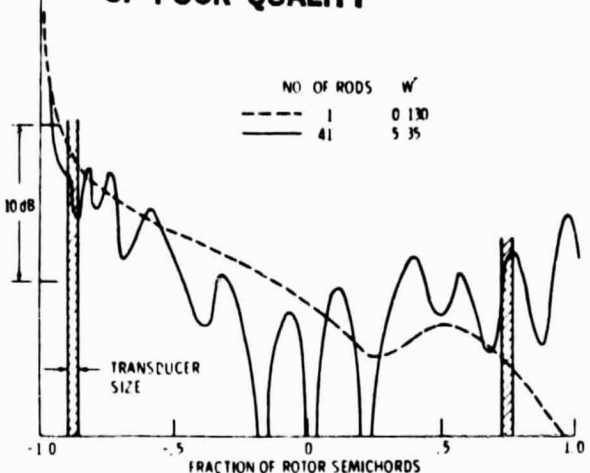


Figure 13. - Calculated chordwise variation of the fundamental component of rotor blade pressure generated by wakes from upstream rods.

trailing edges. For high disturbance frequencies the analysis indicates that measured blade pressure amplitudes are subject to uncertainty due to finite transducer size and sensitivity to transducer location. However, experimental checks of the cascade response analysis using carefully controlled flow disturbances are needed.

Rotor-Stator Interaction. To apply the cascade response analyses just described to one of the main tone noise generation mechanisms, rotor-stator interaction, a thorough description of the rotor produced disturbance flow field is required. The need to describe blade wakes has long been recognized and a large body of wake data including mean and turbulence properties has been accumulated on laboratory fans (e.g., 42, 43). In addition to mid-span wakes, secondary flows such as tip vortices have been recognized as potential noise contributors (44). Therefore, a linear cascade analysis including spanwise gust components has been developed to allow the relative noise contributions of tip vortices and mid-span wakes to be determined (45). What is lacking is a thorough model of the total rotor downstream flow field which is linked to fan design parameters and is validated by experimental data.

Some wake data have been obtained as functions of downstream distance on a fan operated with forward velocity in an anechoic wind tunnel (46). Mean wake stator upwash velocity profiles are shown in Fig. 14 as a function of spanwise position. The magnitudes vary substantially with radial location, but most significantly the profile near the tip is characterized by an extra upwash cycle between successive blades corresponding to strong secondary flows, probably a tip vortex. The variation of stator upwash harmonics, the required input to generation analyses, are shown in Fig. 15 as a function of downstream distance. From the complex variations observed, it must be concluded that simple Gaussian profiles which decay and spread monotonically with distance are an inadequate description of this flow field.

Acoustic data are available from rotor-stator spacing experiments on the same fan as was used for the wake measurements just described. Two stator vane-rotor blade ratios were examined: one for propagating and the other for cutoff fundamental tones. Figure 16 shows the inlet narrowband tone harmonic power level variation with rotor-stator spacing. Residual levels of the fundamental for the cutoff case (25 vanes) are

ORIGINAL PAGE IS  
OF POOR QUALITY

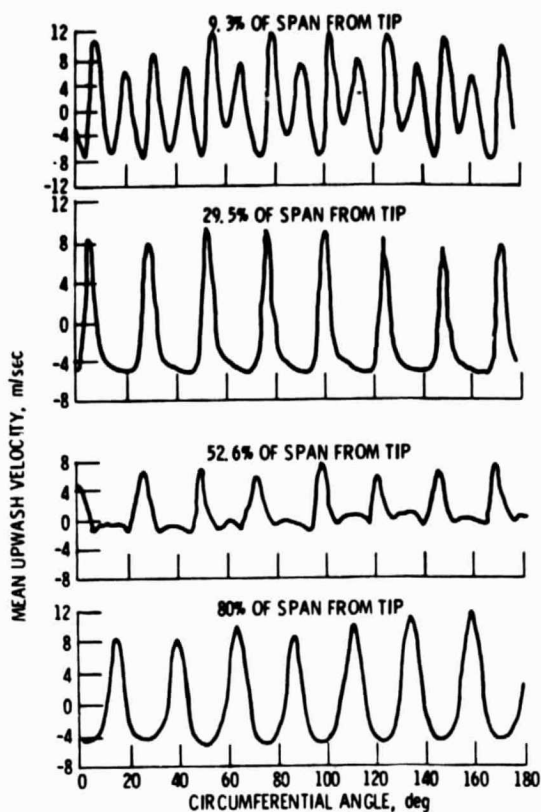


Figure 14. - Rotor mean wake velocity profiles as a function of spanwise location, 1.23 rotor chords downstream, 80% design speed, tunnel vel. = 41 m/sec. (Ref. 46)

nearly constant suggesting that a weak inflow disturbance-rotor interaction governs in this case rather than a rotor-stator interaction due to stator blade non-uniformities sufficient to generate other propagating modes (48). Note that 25-vane second and third harmonic levels are higher than corresponding harmonic generated by the 11-vane set indicating a difference in the response and/or coupling to acoustic modes of the two stators. The 11-vane stator had longer chords than the 25-vane stator in order to maintain the same solidity. Comparisons between the measurements and theory in Ref. 40 are in progress using the corresponding wake measurements as input. Tone powers measured in rotor-stator spacing and vane-blade ratio experiments in an anechoic chamber using inflow control have been compared to a 2-D (strip) model with encouraging results (49). Wake data were not acquired so a wake model was used. While 2-D theory may do relatively well for power predictions; calculating far field directivity and, therefore, acoustic mode content requires more sophistication in handling duct geometry and, probably, in describing the wake/vortex flow field.

Source Modal Content. Both the magnitudes and phases of all the acoustic modes generated are the fundamental inputs to propagation analyses. To date, most available mode information is much less complete. For tone sources circumferential mode numbers may be determined from rules about blade row interactions (50). No such simple rules exist for radial mode numbers. For example, in rotor-stator interactions the rotor wakes become increasingly radially skewed with downstream distance; one wake may simultaneously

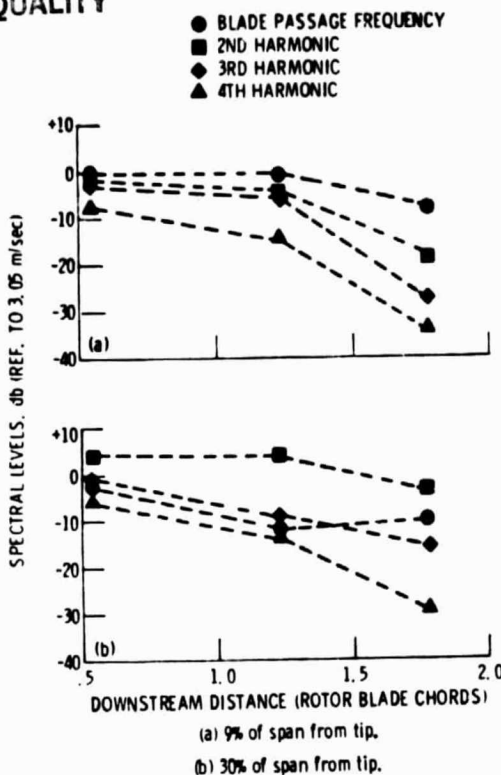


Figure 15. - Mean wake harmonic levels from ensemble average spectra, 80% design speed, upwash component, tunnel vel. = 41 m/sec. (Ref. 46)

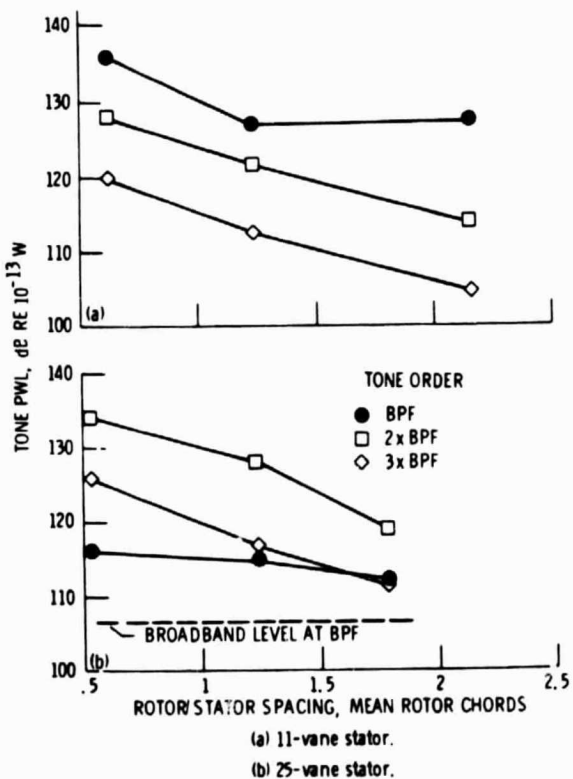


Figure 16. - Variation of narrowband tone harmonic power levels with rotor-stator spacing, 80% design speed, 15 rotor blades, tunnel velocity = 41 m/sec. (Ref. 47)

**ORIGINAL PAGE IS  
OF POOR QUALITY**

intersect several blades with the intersection points sweeping radially with time. In multimodal situations corresponding to random flow excitation, all possible modes that the duct can support are candidates.

Experimentally, two approaches to mode identification have been used. In the first, modal content is inferred from far field directivity. Individual principal mode shapes obtained from radiation theory are matched to the observed lobe shapes (51,52). This method ignores any phasing effects between modes in the far field, depends on the accuracy of the radiation model and breaks down for individual modes as the number of propagating modes increases. In the limit where a large number of modes propagate and a smooth directivity pattern results, either equal amplitude or equal energy modal distributions have been assumed and compared to data. One such study indicated that the equal energy assumption produced a better fit to inlet tone directivities than equal amplitude (53); in another study (54) the equal energy assumption gave fair fits to the multimodal directivities in some cases but poorer results in others, particularly at aft angles.

The second experimental approach has involved attempts at direct mode determination from in-duct microphone measurements. Techniques range from matrix inversion of N selected wall pressures measurements to deterministically solve for N preselected modes (55), to a least-squares approach where the number of measurements is at least twice the number of modes (56). Formidable practical difficulties exist: radial measurements upstream of the fan introduce distortions and their associated extraneous modes, and measurements on the wall alone require large numbers of microphones distributed axially and circumferentially. Demonstrations of the techniques have been limited to relatively low speed fans with conditions rather far removed from the turbofans of interest. Direct measurement techniques require additional development and still fall in the category of research efforts, not routine tools. Thus, results from 3-D or quasi 3-D analyses (35, 36, 40, 41) are presently the main source of detailed modal information.

#### PROPAGATION AND RADIATION - UNLINED DUCTS

In this section we deal with propagation in and radiation from ducts with hard walls. Untreated cases are important for carrying generation predictions to the far field to compare with experiments. Treated ducts will be discussed in the next section.

#### Blade Row Transmission

Sound generated by pressure fluctuations on the stator can only propagate upstream by traversing the rotor and vice-versa. Inlet levels of propagating rotor-stator interaction tones sometimes display low sensitivity to rotor-stator spacing (51, 57) indicating substantial rotor attenuation. Stator generated modes incident on the rotor may be scattered into modes at other blade passing harmonics (58) or sum and difference tones in multistage arrangements (59), and are more highly attenuated if they are rotating opposite to the rotor. While actuator disk (60) and cascade analyses (61) exist, quantitative experimental verification has been limited to two-dimensional approximations (62). The existing analytical framework remains to be applied to 3-D transmission in annular ducts for practical cases where the tone wavelengths of interest are often equal to or less than the blade chords.

#### Inlet Radiation

Assuming any blade row transmission effects have been accounted for, the modal content propagates to

the far field through variable area ducts carrying flow and radiates from duct openings through non-uniform flow fields. For inlet radiation two distinct flow fields are of interest: largely radial potential flow in the static test case, and an inlet stream tube only slightly larger than the inlet diameter in the flight case. The Wiener-Hopf technique, applicable only to inlet lips of negligible thickness, has been applied to two idealized cases. One is uniform external and internal flow at the same Mach number, and the other is a constant Mach number external flow bounding a cylinder of higher uniform Mach number extending out of the inlet. The former is an approximation to the flight case but the latter is unrepresentative of any real inlet flow. Two other approaches to analyzing inlet radiation have been followed. The first uses simplifying assumptions based on ray acoustic while the second uses a fully numerical solution incorporating the actual flow field and inlet lip geometry.

Ray Acoustics in Terms of Cutoff Ratio. Approximate expressions for inlet radiation have been developed in terms of mode cutoff ratio  $\xi = \pi n / a_{mn} \sqrt{1 - M_D^2}$  where the dimensionless frequency  $n = f D/c$ ; with the eigenvalue of the  $(m,n)$ th mode,  $a_{mn}$ ; duct diameter,  $D$ ; duct Mach number,  $M_D$ ; and speed of sound,  $c$ . The key simplification realized by the cutoff ratio formulation is that modes with the same  $\xi$  and  $n$  propagate similarly to the far field. This has been demonstrated for radiation from a flanged duct without flow (63) and is fairly accurate for principal lobe radiation (64). Two important duct mode propagation angles,  $\phi_x$  and  $\psi_x$ , are defined in (65) as

$$\cos \phi_x = \frac{-M_D + S}{1 - M_D S} \quad (1)$$

and

$$\cos \psi_x = \frac{S \sqrt{1 - M_D^2}}{\sqrt{1 - M_D^2 S^2}} \quad (2)$$

where

$$S = \sqrt{1 - 1/\xi^2} \quad (3)$$

Here,  $\phi_x$  and  $\psi_x$  are the angles which the vector normal to the wave front and the group velocity vector, respectively, make with the duct axis. The duct mode angle  $\psi_x$ , given by Eq. (2), has been shown to closely approximate the angular location of the principal lobe in the far field (65). This conclusion was reached by inspection of the directivity coefficient appearing in the Wiener-Hopf solution for the case of uniform flow everywhere (66); an expression for the principal lobe angle identical to Eq. (2) was obtained. The approximate equality of in-duct propagation angle and far field principal lobe radiation angle suggests that ray acoustics arguments can be used to link the two angles for cases where the flow is not uniform.

For example, ray acoustics ideas have been applied to the case where far field velocity is substantially less than inlet duct velocity, the limit being the static case where far field velocity is zero. Based on a ray acoustics analysis which showed that refraction in a potential flow is of second order in Mach number (67), the wavefronts were assumed to be unbent going from duct to far field. That is,  $\phi_x$  was assumed to be unchanged. Since  $\phi_x$  and  $\psi_x$  are identical if Mach number is zero, the group velocity in the far field was assumed to have been shifted. At  $M_D = -0.4$  and  $\xi \approx 1$  (near cutoff), the calculated radia-

# ORIGINAL PAGE IS OF POOR QUALITY

tion peak is at  $66^\circ$  while the group velocity in the duct propagates at  $\psi_x = 90^\circ$ . A peak near  $66^\circ$  was observed in the far field for a nearly cutoff mode generated by a controlled fan source (52). However, the agreement of this observed peak with the theory which neglects lip shape may be misleading. A propagation phenomenon associated with the very thick inlet lip used in the experiment may have controlled the principal lobe location. An analysis of propagation in a variable area duct with gentle area variation shows that mode identity is preserved (68, 69) (i.e., no scattering occurs). Thus, as a mode propagates from the inlet throat to the highlight,  $\xi$  increases causing  $\phi_x$  and  $\psi_x$  to decrease. Recent extensions of ray theory for propagation through an irrotational flow (70, 71) imply that it is the group velocity vector which is unchanged, not the normal to the wavefronts. The difference between the two assumptions is significant; e.g.,  $66^\circ$  vs.  $90^\circ$  peak near cutoff, and current evidence points to preservation of group velocity as the better approach. Controlled experiments and possibly numerical simulations are needed to settle this issue.

Numerical Model. A hybrid numerical program has been developed (72) and exercised (73) to calculate both the internal and external sound propagation for actual engine inlet geometry and flow conditions. It is a hybrid program in the sense that a finite element method is used within the duct and in the near field and an integral radiation method handles the far field. Iteration is required to match the two solutions at the interface. A potential flow program is used to generate the steady flow for the actual inlet geometry; boundary layers are not included. The input to the program is the pressure profile for a given mode in the annulus at the fan source. While the program cannot handle the combination of high Mach number and high frequency due to computer storage limitations, some inlet geometry effects have been studied which were previously impossible to analyze.

Figure 17 compares the numerically predicted inlet tone directivity to the measured levels generated by the same controlled source mentioned previously--a JT15D engine with inlet rods (52). A single (13,0) mode propagates at the fan speed shown. The excellent agreement between the hybrid solution and the data is in contrast to the Wiener-Hopf solution for an infinitely thin lip, which is also shown. The thick lip used in the experiment (thickness-to-diameter ratio of 0.5) shifts the radiation peak toward the axis, as

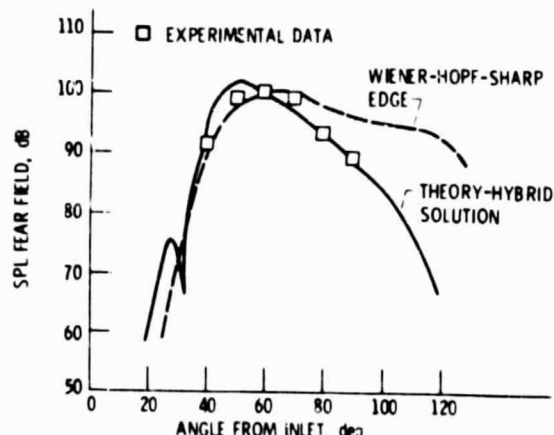


Figure 17. - Single mode inlet directivity comparison of theory with experiment 3150 Hz, (13,0) mode. (Ref. 85)

discussed in the preceding section, and acts as a shield to reduce the levels in the aft quadrant. The dependence of the directivity on inlet lip thickness is illustrated in Fig. 18 where the shielding effect is also clearly evident. The numerical results show that the radiation peak moves aft as the lip gets thinner. At a thickness-to-diameter ratio of 0.1, the radiation pattern agrees very well with the Wiener-Hopf (zero thickness) result shown in Fig. 17. The hybrid program is a powerful tool for the solution of "real-world" inlet radiation problems.

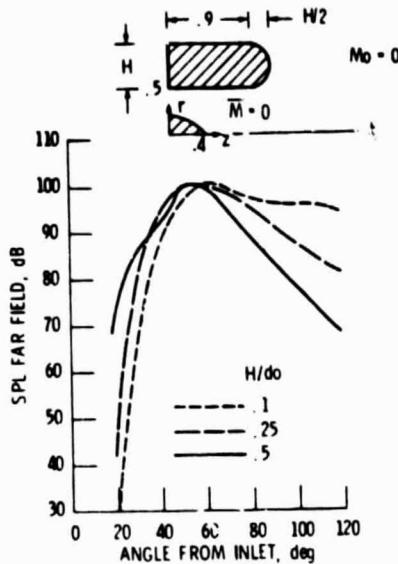


Figure 18. - Effect of inlet lip thickness on single mode directivity,  $M_D = 0$ , 3150 Hz (13,0) mode, (theory normalized to 100 dB at  $60^\circ$ ). (Ref. 85)

#### Exhaust Radiation

In contrast to the complex inlet flow field, the exhaust flow, neglecting mixing, is much simpler. The fan exhaust may be approximated as an emerging cylindrical flow at Mach number  $M_f$  surrounded by a uniform flow at Mach number  $M_e$  which fits the requirements for an exact Wiener-Hopf radiation solution. The ray acoustics, mode cutoff ratio approach to an approximate solution can also be applied with more confidence to the aft slip layer. Starting from the zero-flow flanged duct radiation equation, a coordinate transformation was applied to account for the duct flow, and ray acoustics arguments were applied across the slip layer (74). Single mode aft directivity from the approximate expression is compared to the full Wiener-Hopf solution (75) in Fig. 19. The good agreement builds confidence in the simplifications used to generate the approximate solution. The Wiener-Hopf solution gives finite levels in the zone of silence in contrast to the ray acoustics result although the particular values from (75) are believed to be incorrect.

The location of the principal lobe in the far field,  $\psi_{fp}$ , is found from the approximate theory (74) to be:

$$\cos \psi_{fp} = \frac{-M_f + \xi \sqrt{\xi^2 - 1} (1 - M_f^2)}{(1 - M_f^2)^2 (\xi + M_f \sqrt{\xi^2 - 1})} \quad (4)$$

for the static case ( $M_f = 0$ ). For  $M_f = +0.6$  and  $\xi = 1$ ,  $\psi_{fp} = 160^\circ$  measured from the exhaust axis indicating that modes near cutoff radiate to the inlet quadrant.

# ORIGINAL PAGE IS OF POOR QUALITY

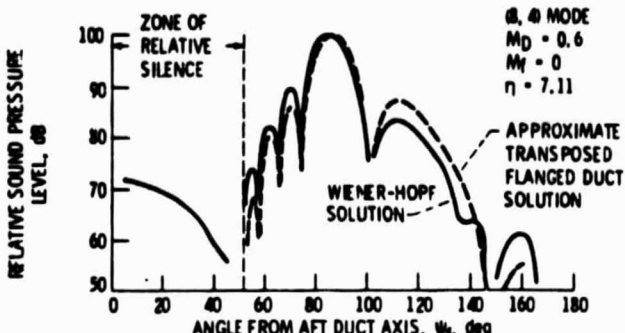


Figure 19. - Comparison of approximate and exact single mode aft directivity patterns. (Ref. 74)

rant. The analogous inlet analysis, Eq. (2), indicated that near cutoff mode peaks remain in the inlet quadrant. Thus, the inlet quadrant contains the near cutoff mode peaks no matter where the sound originated.

#### SUPPRESSION - LINED DUCTS

Ducts between the turbomachinery components and the observer can be lined with sound absorbing materials to greatly reduce the radiated noise. Early workers (77) on suppressors considered the use of splitter rings in the duct to increase treated area and decrease the distance between treated surfaces.

Current emphasis is on the optimization of wall treatment alone to minimize aerodynamic losses and weight penalties in aircraft applications. The attenuation achieved is very sensitive to the source modal characteristics used as input (78, 79). Input cases of interest range from a limited number of modes associated with tone noise from periodic blade row interactions, to multi-modal situations associated with random processes exciting all the modes the duct can support. The latter number may be very large. At high frequencies considering modes spinning in one direction, the number can be estimated from Ref. (80) as  $N = \pi^2 n^2 / 8(1 - M_D^2)$ . For typical values of  $M_D = -0.4$  and  $n = 20$  at blade passing frequency,  $N \approx 600$ . In such cases, some method of handling the modal distribution as a continuum subject to a simple rule describing the energy distribution is desirable.

The status of three aspects of suppressor research will be discussed: analytical propagation approaches including the cutoff ratio method, numerical propagation programs, and suppressor materials characterization.

#### Duct Acoustics - Analytical

Much analytical effort has gone into describing propagation of acoustic modes in simple geometries such as cylindrical and rectangular ducts lined with sound absorbing materials. A complex acoustic impedance (resistance and reactance) is used to specify the wall boundary condition for point reacting liners. Solution of the wave equation in the duct results in a complex eigenvalue and wave number for each mode. The real part of the wave number defines the attenuation while the imaginary part defines the axial wave speed.

From such single mode solutions, attenuation contours plotted in the impedance plane, as shown in Fig. 20, reveal an optimum impedance for which the maximum possible attenuation is obtained. The important parameters are duct Mach number, boundary layer thickness and frequency. Studies of optimum impedance led to the discovery (81) that mode cutoff ratio was a key

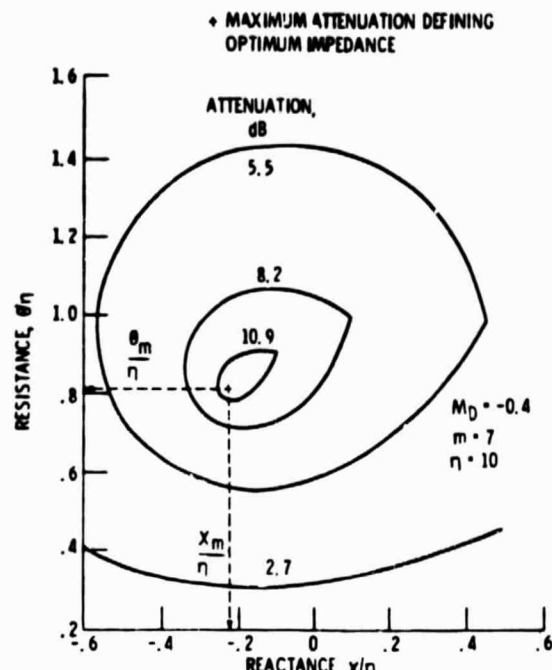


Figure 20. - Sound attenuation contours boundary layer thickness  $\epsilon = 0$ ; liner length/passage height,  $U/H = 1.0$ . (Ref. 82.)

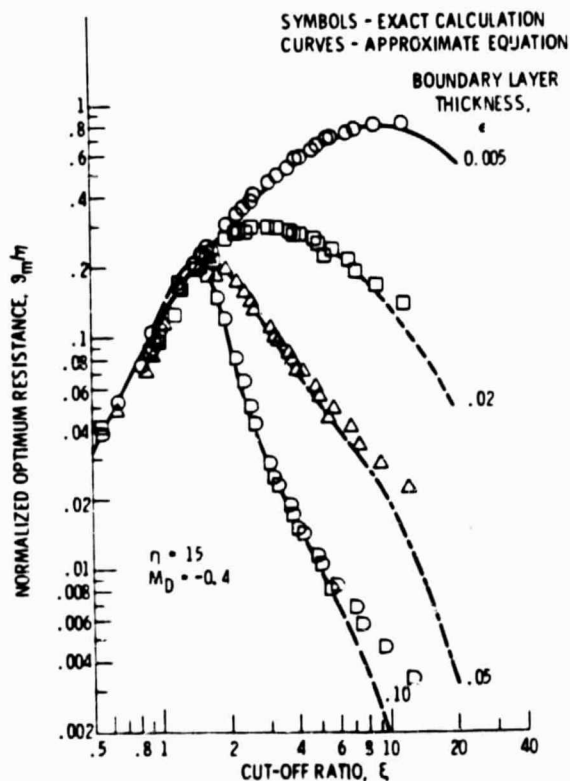


Figure 21. - Optimum wall resistance as a function of mode cutoff ratio for various inlet wall boundary layer thicknesses. (Ref. 82)

correlating parameter: modes with similar cutoff ratios propagate in a similar fashion. Figure 21 shows the correlation of optimum resistance as a function of cutoff ratio for different boundary layer

# ORIGINAL PAGE IS OF POOR QUALITY

thicknesses. Each point represents a single mode calculation. The curves through the points are from a correlation equation reported in Ref. (82) which also contains correlations for maximum possible attenuation and optimum reactance. Highest attenuation occurs near cutoff and drops rapidly with increasing cutoff ratio. Cutoff ratio correlations have been found for far field directivity (63) duct termination loss (63) and transmission loss through a variable area duct based on  $\xi$  at the throat (68, 69).

Multimodal cases, such as the example of  $N = 600$  cited above, can be handled as a continuum in cutoff ratio. The modal number density function in a duct is given in (80) by:

$$\frac{1}{N} \frac{dN}{d\xi} \approx \frac{2}{\xi^3} \quad (5)$$

The number density is converted into a modal power density by multiplying by a weighting function which must then be estimated by a technique such as a least squares fit to experimental hardwall directivity patterns as described in Ref. (6).

The goal of these approximate suppressor analyses is to predict the suppressed far field directivity. Additional work is needed to improve the quantitative results by including modal scattering at the hard-soft liner interface, refraction around the inlet lip at high Mach number and redirection of sound by the inlet lip contour. Analogous optimum impedance and attenuation correlations remain to be derived for the aft duct case.

#### Duct Acoustics - Numerical

Recent reviews of the application of numerical methods to duct acoustics appear in Refs. (83) and (84). The hybrid numerical program in the "Inlet Radiation" section also handles the case of acoustically treated inlet walls. Comparisons of the calculated and measured suppression for a series of very short inlet liners ( $L/D = 0.15$ ) are shown in Fig. 22 (85). The experiment again used a JT15D engine configured to

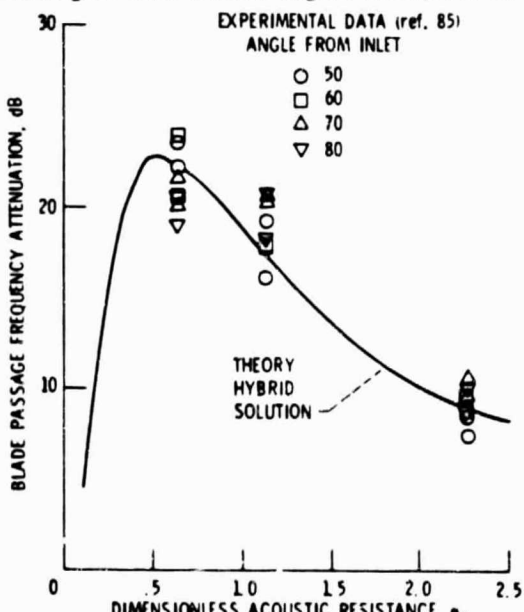


Figure 22. - Comparison of numerical suppression/radiation analysis to experiment as a function of liner resistance (13,0) mode, 3150 Hz,  $x = 0.5$ . (Ref. 85)

produce a single (13,0) mode. Three different liner resistances were tested (86). For a single mode the attenuation is independent of angle. Therefore, at each resistance, data points are plotted for angles between  $50^\circ$  and  $80^\circ$  where the single mode at blade passing frequency dominates the levels. The calculated values agree well with the data which vary less than 5 dB with angle.

The hybrid program has been used to calculate attenuation contours in the impedance plane and thus define the optimum impedance (85) for the single mode as shown in Fig. 23. Optimum values of resistance and reactance are 0.6 and 0.85 compared to values of 1.14 and 0.5 calculated for a single (13,0) mode in the soft-walled duct. Corresponding maximum possible attenuations differ by 20 dB (50 dB numerical vs. 30 dB single mode). These comparisons show the importance of the inclusion in the hybrid program of modal scattering at the hard-soft interface, particularly for a near cutoff mode entering a short liner. As the liner is lengthened, the numerical calculation approaches the analytical result which neglects scattering. A semi-empirical correction was applied in Ref. (85), but explicit inclusion of scattering in the analysis is preferable.

The challenge in applying the numerical approach is to remove the limitations on frequency and Mach number ranges imposed by computer storage and run time. One possibility is to develop a transient solution method which can potentially cut storage requirements by several orders of magnitude (87, 88).

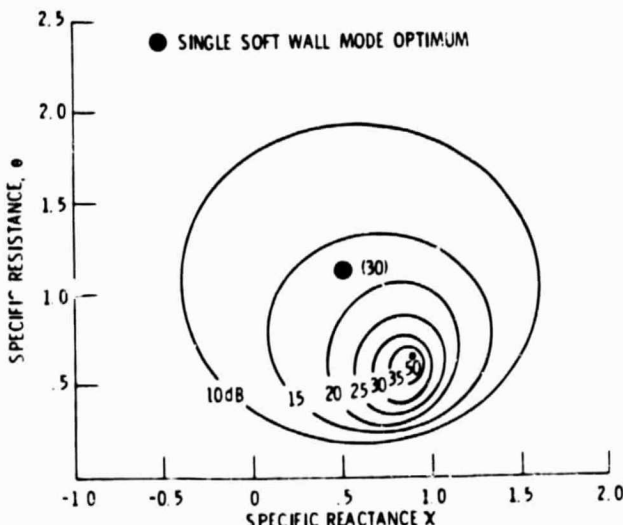


Figure 23. - Calculated optimum impedances from a hybrid numerical solution with scattering compared to the single soft wall mode solution, 3150 Hz (13,0) mode, liner  $L/d = .15$ . (Ref. 85)

#### Suppressor Materials

In order to realize the attenuations calculated by the propagation analyses, the duct boundary conditions expressed as acoustic impedance must be translated into liner construction parameters, e.g., treatment thickness, wall porosity, fiber sizes and bulk densities, etc. For extended reaction liners, normal wall impedance is inappropriate and coefficients in the wave equation describing propagation in the liner itself must be related to real bulk absorbing material properties. The following discussion will briefly summarize the physics of the various dissipation mechanisms involved and some recent modelling efforts to link the suppressor construction details to the global properties needed for propagation analysis.

Impedance - Point Reacting Materials. Helmholtz resonator arrays formed by bonding a perforated plate to honeycomb have been widely used to acoustically treat aircraft engine ducts. In the absence of the grazing flow present in engine applications, these suppressors are extremely non-linear, i.e., resistance depends on sound pressure level because the oscillatory orifice flow is governed by the Bernoulli equation. However, at high grazing flows the resistance is proportional to free stream Mach number and is independent of sound pressure level. The control of resistance by grazing flow is due to orifice blockage which occurs as the mean flow is periodically turned into the orifices and then separates, reducing the discharge coefficients or the effective open area ratio of the perforated plate (89). Acoustic dissipation occurs as the kinetic energy of the hydrodynamic jet-like flow induced in the orifices is dissipated in the surrounding fluid with little pressure recovery. Actually, boundary layer properties must also be considered since the orifices ingest flow from distances of the order of one orifice diameter. Acoustic resistance models have been published (86,90) as a function of free stream Mach number and boundary layer thickness based on a 1/7th power profile. Recently, a model using friction velocity as the controlling parameter has been formulated (91) to handle the more general case of a boundary layer thickened by diffusion or altered in a way which deviates near wall velocities from free stream conditions.

Perforated plate-honeycomb treatment has cost and load carrying advantages, but its acoustic design is complicated by the requirement to know local flow conditions which vary with engine speed. (The associated resistance variation is favorable in an inlet but detrimental in the exhaust). To overcome the sensitivity of resistance to flow conditions and maintain acoustic linearity, treated surfaces having very small pores formed by densely packed wires or extremely fine screens have been used. In this case, the dissipation mechanism is viscous pressure loss in the fine pores as nearly stagnant fluid very near the wall is ingested. An impedance model for square weave screens supported by perforated plate has been developed (92). Mechanical problems associated with fine screens have been addressed. Corrosion at the bonds with dissimilar metals can be prevented with coatings. Contamination is prevented by the self-cleaning action of the oscillatory velocities induced in the pores. Aside from the increased in situ impedance predictability, fine-pored materials have no acoustic advantage over perforated plate when used in a honeycomb-backed wall treatment.

Bulk Absorbers. Extended reaction liners formed by an uninterrupted layer of densely packed fibers retained by a high porosity face sheet do offer definite acoustic advantages. The distributed dissipation damps back cavity resonances which smooths the reactance as a function of frequency and increases high frequency absorption.

At low frequencies the speed of sound in the fibrous matrix is decreased giving a greater apparent treatment depth and enhancing low frequency absorption. Beyond these inherently point reacting arguments, the possibility that axial and circumferential wave travel in the material may be used to advantage is being investigated (93). Studies of the effects of high sound intensities on bulk absorber properties have been completed (94) and models for a range of bulk absorber types are under development (95).

There are mechanical difficulties associated with

extended reaction liners which must be overcome. Absorption of liquids will destroy the acoustic effectiveness and can pose a safety problem. Non-wetting coatings may solve the problem for some liquids and allow removal of others using compatible solvents. To provide structural strength while preserving extended reaction, porous (acoustically-transmitting) axial and circumferential face plate supports may be required.

#### CONCLUDING REMARKS

##### Status and Outlook

This review has addressed the links in the chain of aeroacoustic processes which connect turbofan noise generation and suppression to the observed far field noise. Although the theoretical outlines and a body of often flawed empirical data have been in hand for a decade or more, the unified application of theory and controlled experiment to practical cases is just now occurring. This productive development was delayed by contaminated data and theoretical complexity whose physical implications were inadequately communicated to or assimilated by applied noise researchers. During the past half decade, key advances have been made in experimental technique and theoretical application which open the way to a much broader understanding and control of turbofan noise.

With respect to generation, the development of effective inflow control techniques makes possible the conduct of definitive experiments on internally controlled blade row interactions. The initial round of such experiments, focused on rotor-stator tone generation, has highlighted the question of the relative importance of secondary flow disturbances (e.g., tip vortices) compared to mid-span wakes. Both improved descriptions of the rotor-produced flow disturbances and the noise generation computer codes to use them are being developed to answer this question. With the help of rotor blade pressure measurements and inflow control, rotor interaction with struts downstream of the stator has been identified as a significant noise source. The experimental tools now exist to uncover other such mechanisms which set tone levels in specific engines. Computer codes which incorporate non-compact, cascade response to calculate the generated acoustic mode content are in the process of being validated by experiment. Tone power comparisons show good agreement. The next level of validation involves far field directivity which depends on a prediction of individual modes and their propagation behavior. At least a quasi-3D calculation approach must be used to give both circumferential and radial mode content.

Pending the development of well-proven modal measurement techniques, confirmation of predicted mode content is intertwined with hardwall propagation and radiation analysis. The theoretical approaches discussed include approximate analyses, Wiener-Hopf techniques and direct numerical solutions. Geometric acoustics approximations cast in terms of mode cutoff ratio have the advantage of producing relatively simple expressions and rules of thumb. The cutoff ratio combines individual mode identity (eigenvalue) with frequency and Mach number in a parameter which is particularly convenient for handling multimodal cases as a continuum. Aft fan radiation appears to be handled well by these techniques, but the geometric acoustics of the inlet lip and potential flow field require additional work. On the other hand, the realistic inlet lip geometry and flow field can be accounted for by direct numerical methods such as the hybrid code. The challenge is to remove the computer storage limitations on combined frequency and flow range.

# ORIGINAL PAGE IS OF POOR QUALITY

The approximate analytical and the full numerical approaches also bracket the range of suppressor analyses. Cutoff ratio is again a very useful parameter correlating the attenuation and optimum wall impedance in lined ducts. The results from a full numerical solution, the hybrid code, have particularly emphasized the importance of modal scattering at the hard-soft interface for short treatment lengths. For the multimodal situation resulting from random generation processes, the key input to suppressor analysis is the modal energy distribution. While some broadband cases appear to follow equal energy, in general, the distribution must be inferred by empirical fits to data. The generation models now coming into use may provide some analytical guidance in this regard. The ability to specify acoustic treatment construction has been strengthened by improved understanding of the absorption physics which is concretely reflected in improved impedance models particularly for Helmholtz resonator arrays in flow environments. The quest for wider absorption bandwidth and enhanced low frequency attenuation for a given treatment depth spurs the continued investigation of bulk absorbers in full extended reaction configurations.

## Other Turbomachinery Installations

Several research results highlighted in this review are relevant to the noise control of stationary turbomachinery. The importance of reducing inflow disturbances to rotating blade rows, particularly for tone noise reduction, and the inflow control devices demonstrated for turbofans apply to stationary cases. In contrast to the turbofan testing constraint, in-duct honeycomb devices are an option. The recent finding that strong tones can be generated by downstream structural struts which interact with upstream rotors through intervening stators is another example of a mechanism likely to be generally operative. Blade pressure diagnostics represent a helpful tool for such mechanism identification. Duct acoustic treatment can be effectively applied to produce a compact suppressed installation. The approximate design methods based on cutoff ratio may be particularly helpful for multimodal situations that are likely to arise in complex, multistage machines.

## REFERENCES

1. Owens, R. E., "Energy Efficient Engine Propulsion System - Aircraft Integration Evaluation," NASA CR-159488, March 1979.
2. Johnston, R. P., et al., "Energy Efficient Engine - Preliminary Design and Integration Study," NASA CR-135444, Sept. 1978.
3. Hodge, C. G., "Subsonic Transport Noise," AIAA Paper 80-0858, May 1980.
4. Cumpsty, N. A., "A Critical Review of Turbomachinery Noise," *Trans. ASME J. of Fluids Engineering*, Vol. 99, No. 2, June 1977, pp. 278-293.
5. Feiler, C. E., and Groeneweg, J. F., "Summary of Forward Velocity Effects of Fan Noise," AIAA Paper 77-1319, Oct. 1977 (also NASA TM 73722).
6. Rice, E. J., and Sawdy, D. J., "A Theoretical Approach to Sound Propagation and Radiation for Ducts with Suppressors," Presented at the 101st Meeting of the Acoustical Society of America, Ottawa, Ont., Can., May 1981 (also NASA TM 82612).
7. Dean, L. W., and Patrick, W. P., "Impedance Modeling of Acoustic Absorbing Materials for Aircraft Engine Applications," Paper X5 presented at the 101st Meeting of the Acoustical Society of America, Ottawa, Ont., Can., May 1981.
8. Hanson, D. B., "Spectrum of Rotor Noise Caused by Atmospheric Turbulence," *Journal of Acoustical Society of America*, Vol. 56, July 1974, pp. 110-126.
9. Tyler, J. M., and Sofrin, T. G., "Axial Flow Compressor Noise Studies," *SAE Transactions*, Vol. 70, 1962, pp. 309-332.
10. Sofrin, T. G., and McCann, J. F., "Pratt and Whitney Experience in Compressor-Noise Reduction," Abstracted in *Journal of Acoustical Society of America*, Vol. 40, 1966, pp. 1248-1249.
11. Jones, W. L., McArdle, J. G., and Homyak, L., "Evaluation of Two Inflow Control Devices for Flight Simulation of Fan Noise Using a JT15D Engine," AIAA Paper 79-0654, March 1979 (also NASA TM 79072).
12. McArdle, J. G., Jones, W. L., and Heidelberg, L. J., "Comparison of Several Inflow Control Devices for Flight Simulation of Fan Noise Using a JT15D Engine," AIAA Paper 80-1025, June 1980 (also NASA TM 81505).
13. Woodward, R. P., et al., "Effectiveness of an Inlet Flow Turbulence Control Device to Simulate Flight Fan Noise in an Anechoic Chamber," NASA TM 73855, Dec. 1977.
14. Chestnutt, D. (editor), "Flight Effects of Fan Noise," NASA CP 2242, Sept. 1982.
15. Loehrke, R. I., and Nagib, H. M., "Control of Free Stream Turbulence by Means of Honeycombs: A Balance Between Suppression and Generation," *Journal of Fluids Engineering*, Vol. 98, Sept. 1976, pp. 342-353.
16. Rogers, D. F., and Ganz, U. W., "Aerodynamic Assessment of Methods to Simulate Flight Inflow Characteristics During Static Engine Testing," AIAA Paper 80-1023, March 1980.
17. Kantola, R. A., and Warren, R. E., "Reduction of Rotor-Turbulence Interaction Noise in Static Fan Noise Testing," AIAA Paper 79-0656, March 1979.
18. Ho, P. Y., and Smith, E. B., "An Inflow Turbulence Reduction Structure for Scale Model Fan Testing," AIAA Paper 79-0655, March 1979.
19. Ginder, R. B., "Considerations for the Design of Inlet Flow Conditioners for Static Noise Testing," AIAA Paper 79-0657, March 1979.
20. Ganz, U. W., "Analytical Investigation of Fan Tone Noise Due to Ingested Atmospheric Turbulence," NASA CR 3302, Aug. 1980.
21. Gedge, M. R., "A Design Procedure for Fan Inflow Control Structures," NASA CR 165625, Sept. 1980.
22. Atvars, Y., and Rogers, D. F., "The Development of Inflow Control Devices for Improved Simulation of Flight Noise Levels During Static Testing of a HBPR Turbofan Engine," AIAA Paper 80-1024, June 1980.
23. Perracchio, A. A., "Assessment of In-Flow Control Structure Effectiveness and Design System Development," AIAA Paper 81-2048, Oct. 1981.
24. Shaw, L. M., et al., "Inlet Turbulence and Fan Noise Measured in an Anechoic Wind Tunnel and Statically with an Inlet Flow Control Device," AIAA Paper 77-1345, Oct. 1977 (also NASA TM 73723).
25. Heidmann, M. F., and Dietrich, D. A., "Effects of Simulated Flight on Fan Noise Suppression," AIAA Paper 77-1334, Oct. 1977.
26. Holm, R. G., Langenbrunner, L. E., McCann, E. O., "Forward Velocity Effects on Fan Noise and the Influence of Inlet Aeroacoustic Design as Measured in the NASA-Ames 40x80 Foot Wind Tunnel," NASA CR 152329, July 1981.
27. Ho, P. Y., "The Effect of Fan-Frame Design on Rotor-Stator Interaction Noise," AIAA Paper 81-2034, Oct. 1981.

**ORIGINAL PAGE IS  
OF POOR QUALITY**

- 81-2034, Oct. 1981.
28. Ginder, R. B., and Newby, D. R., "An Improved Correlation for the Broadband Noise of High Speed Fans," *AIAA Journal of Aircraft*, Vol. 14, No. 9, Sept. 1977, pp. 844-849.
  29. Giesebe, P. R., "The Effect of Throttling on Forward Radiated Fan Noise," *AIAA Paper 79-0640*, March 1979.
  30. Hayden, R. E., et al., "Analysis and Design of a High Speed, Low Noise Aircraft Fan Incorporating Swept Leading Edge Rotor and Stator Blades," *NASA CR 135092*, Feb. 1978.
  31. Lucas, J. G., Woodward, R. P., and MacKinnon, M. J., "Acoustic Evaluation of a Novel Swept-Rotor Fan," *AIAA Paper 78-1121*, July 1978.
  32. Lucas, J. G., Woodward, R. P., and Michels, C. J., "Forward Acoustic Performance of a Model Turbofan Designed for a High Specific Flow (QF-14)," *NASA TP 1968*, March 1982.
  33. Mathews, D. C., and Nagel, R. T., "Inlet Geometry and Axial Mach Number Effects on Fan Noise Propagation," *AIAA Progress in Astronautics and Aeronautics*, Vol. 38, 1975, pp. 73-96.
  34. Namba, M., "Three-Dimensional Analysis of Blade Force and Sound Generation for an Annular Cascade in Distorted Flows," *Journal of Sound and Vibration*, Vol. 50, Feb. 1977, pp. 479-508.
  35. Kobayashi, H., "Three Dimensional Effect on Pure Tone Fan Noise Due to Inflow Distortion," *AIAA Paper 78-1120*, July 1978 (also NASA TM 78885).
  36. Schulten, J. B. H. M., "A Lifting Surface Theory for the Sound Generated by the Interaction of Velocity Disturbances with a Leaned Vane Stator," *AIAA Paper 81-0091*, Jan. 1981.
  37. Goldstein, M. E., *Aerodynamics*, McGraw-Hill, New York, 1976.
  38. Kaji, S., "Noncompact Source Effect on the Prediction of Tone Noise from a Fan Rotor," *AIAA Paper 75-446*, 1975.
  39. Fleeter, S., "Discrete Frequency Noise Reduction Modeling for Application to Fanjet Engines," *Journal of Acoustical Society of America*, Vol. 63, No. 3, Sept. 1980, pp. 957-965.
  40. Ventres, C. S., Theobald, M. A., and Mark, W. D., "Turbofan Noise Generation," Volume I: Analysis *NASA CR 167951* and Volume II: Computer Programs *NASA CR 167952*, July 1982.
  41. Kobayashi, H., and Groeneweg, J. F., "Effects of Inflow Distortion Profiles on Fan Tone Noise," *AIAA Journal*, Vol. 18, No. 8, Aug. 1980, pp. 899-906.
  42. Reynolds, B., and Lakshminarayana, B., "Characteristics of Lightly Loaded Fan Rotor Blade Wakes," *NASA CR 3188*, Oct. 1979.
  43. Ravindranath, A., and Lakshminarayana, B., "Three Dimensional Mean Flow and Turbulence Characteristics of the Near Wake of a Compressor Rotor Blade," *NASA CR 159518*, June 1980.
  44. Dittmar, J. H., "Interaction of Rotor Tip Flow Irregularities with Stator Vanes as a Noise Source," *AIAA Paper 77-1342*, Oct. 1977 (also NASA TM 73706).
  45. Atassi, H., and Hamad, G., "Sound Generated in a Cascade by Three-Dimensional Disturbances Convected in a Subsonic Flow," *AIAA Paper 81-2046*, Oct. 1981.
  46. Shaw, L. M., and Balombe, J. R., "Rotor Wake Characteristics Relevant to Rotor-Stator Interaction Noise Generation," *AIAA Paper 81-2031*, Oct. 1981 (also NASA TM 82703).
  47. Woodward, R. P., and Glaser, F. W., "Effects of Blade-Vane Ratio and Rotor-Stator Spacing on Fan Noise with Forward Velocity," *AIAA Paper 81-2032*, Oct. 1981 (also NASA TM 82690).
  48. Sofrin, T. G., and Mathews, D. C., "Asymmetric Stator Interaction Noise," *AIAA Paper 79-0636*, March 1979.
  49. Kantola, R. A., and Giesebe, P. R., "Effects of Vane/Blade Ratio and Spacing on Fan Noise," *AIAA Paper 81-2033*, Oct. 1981.
  50. Sofrin, T. G., "Some Modal-Frequency Spectra of Fan Noise," *AIAA Paper 81-1990*, Oct. 1981.
  51. Cumpsty, N. A., "Tone Noise from Rotor-Stator Interaction in High Speed Fans," *Journal of Sound and Vibration*, Vol. 24, No. 3, 1972, pp. 393-409.
  52. Heidmann, M. F., Saule, A. V., and McArdle, J. G., "Predicted and Observed Modal Radiation Patterns from JT15D Engine with Inlet Rods," *J. Aircraft*, Vol. 17, 1980, pp. 493-499.
  53. Saule, A. V., "Modal Structure Inferred From Static Far-Field Noise Directivity," *NASA TMX 71909*, July 1976.
  54. McArdle, J. G., Homyak, L., and Chrulski, D. D., "Turbomachinery Noise Studies of the AIR Research QCGAT Engine with Inflow Control," *AIAA Paper 81-2049*, Oct. 1981.
  55. Pickett, G. F., Sofrin, T. G., and Wells, R. A., "Method of Fan Sound Mode Structure Determination, Final Report," *NASA CR 135293*, Aug. 1977.
  56. Moore, C. J., "Measurement of Radial and Circumferential Modes in Annular and Circular Fan Ducts," *Journal of Sound and Vibration*, Vol. 62, No. 2, 1979, pp. 235-256.
  57. Woodward, R. P., and Glaser, F. W., "Effect of Inflow Control on Inlet Noise of a Cut-on Fan," *AIAA Journal*, Vol. 19, No. 3, March 1981, pp. 387-392.
  58. Mani, R., and Horvay, G., "Sound Transmission Through Blade Rows," *Journal of Sound and Vibration*, Vol. 12, No. 1, 1970, pp. 59-83.
  59. Cumpsty, N. A., "Sum and Difference Tones from Turbomachinery," *Journal of Sound and Vibration*, Vol. 32, No. 3, 1974, pp. 383-386.
  60. Kaji, S., and Okazaki, T., "Propagation of Sound Waves Through a Blade Row. I. Analysis Based on the Semi-Actuator Disc Theory," *Journal of Sound and Vibration*, Vol. 11, No. 3, 1970, pp. 339-353.
  61. Kaji, S., and Okazaki, T., "Propagation of Sound Waves Through a Blade Row. II. Analysis Based on the Acceleration Potential Method," *Journal of Sound and Vibration*, Vol. 11, No. 3, 1970, pp. 355-375.
  62. Philpot, M. G., "The Role of Rotor Blockage in the Propagation of Fan Noise Interaction Tones," *AIAA Paper 75-447*, March 1975.
  63. Rice, E. J., "Multimodal Far-Field Acoustic Radiation Pattern Using Mode Cutoff Ratio," *AIAA Journal*, Vol. 16, 1978, pp. 906-911.
  64. Saule, A. V., and Rice, E. J., "Far-Field Multimodal Acoustic Radiation Directivity," *NASA TM 73839*, 1977.
  65. Rice, E. J., Heidmann, M. F., and Sofrin, T. G., "Modal Propagation Angles in a Cylindrical Duct with Flow and Their Relation to Sound Radiation," *AIAA Paper 79-0183*, Jan. 1979 (also NASA TM 79030, 1978).
  66. Homicz, G. F., and Lordi, J. A., "A Note on the Radiative Directivity Patterns of Duct Acoustic Modes," *Journal of Sound and Vibration*, Vol. 41, 1975, pp. 283-290.
  67. Landau, L. D., and Lifshitz, E. M., *The Classical Theory of Fluids*, Addison-Wesley, Reading, MA, 1962, Rev. 2nd ed., Ch. 7.
  68. Cho, Y. C., and Ingard, K. U., "Closed Form Solution of Mode Propagation in a Nonuniform

- Circular Duct," AIAA Journal, Vol. 20, No. 1, Jan. 1982, p. 39.
69. Cho, Y. C., and Ingard, K. U., "Mode Propagation in Nonuniform Circular Ducts with Potential Flow," AIAA Paper 82-0122, Jan. 1982 (also NASA TM 82776).
70. Cho, Y. C., and Rice, E. J., "High-Frequency Sound Propagation in a Spatially Varying Mean Flow," Journal of Acoustical Society of America, Vol. 70, No. 3, Sept. 1981, pp. 860-865.
71. Amiet, R. K., "Correction of Fan Noise for Effects of Forward Flight." To be published in Journal of Sound and Vibration.
72. Horowitz, S. J., Sigman, R. K., and Zinn, B. T., "An Iterative Finite Element-Integral Technique for Predicting Sound Radiation from Turbofan Inlets in Steady Flight," AIAA Paper 82-0124, Jan. 1982.
73. Baumeister, K. J., and Horowitz, S. J., "Finite Element-Integral Simulation of Static and Flight Fan Noise Radiation from the JT15D Turbofan Engine," NASA TM 82936, Nov. 1982.
74. Rice, E. J., and Saule, A. V., "Far-Field Radiation of Aft Turbofan Noise," NASA TM 81506, 1980.
75. Savkar, S. D., and Edelfelt, I. H., "Radiation of Cylindrical Duct Acoustic Modes with Flow Mismatch," NASA CR 132613, 1975.
76. Savkar, S. D., "Radiation of Cylindrical Duct Acoustic Modes with Flow Mismatch," Journal of Sound and Vibration, Vol. 42, 1975, pp. 363-386.
77. Minner, G. L., and Rice, E. J., "Computer Method for Design of Acoustic Liners for Turbofan Engines," NASA TMX 3317, 1976.
78. Rice, E. J., "Spinning Mode Sound Propagation in Ducts with Acoustic Treatment," NASA TN D-7913, 1975.
79. Motsinger, R. E., Kraft, R. E., Zwick, J. W., "Design of Optimum Acoustic Treatment for Rectangular Ducts with Flow," ASME Paper 76-CT-113, March 1976.
80. Rice, E. J., "Modal Density Function and Number of Propagating Modes in Ducts," NASA TMX 73539, 1976.
81. Rice, E. J., "Acoustic Liner Optimum Impedance for Spinning Modes with Mode Cut-Off Ratio as the Design Criterion," AIAA Paper 76-516, July 1976 (also NASA TMX 73411).
82. Rice, E. J., "Optimum Wall Impedance for Spinning Modes - A Correlation with Mode Cutoff Ratio," Journal of Aircraft, Vol. 16, 1979, pp. 336-343.
83. Baumeister, K. J., "Numerical Techniques in Linear Duct Acoustics - A Status Report," Journal of Engineering for Industry, Vol. 103, Aug. 1981, pp. 270-281.
84. Baumeister, K. J., "Numerical Techniques in Linear Duct Acoustics - 1980-81 Update," NASA TM 82730, Nov. 1981.
85. Baumeister, K. J., "Utilizing Numerical Techniques in Turbofan Inlet Acoustic Suppressor Design," NASA TM 82994, Oct. 1982.
86. Heidelberg, L. J., Rice, E. J., and Homayak, L., "Acoustic Performance of Inlet Suppressors on an Engine Generating a Single Mode," AIAA Paper 81-1965 (also NASA TM 82697).
87. Baumeister, K. J., "Time Dependent Difference Theory for Noise Propagation in a Two-Dimensional Duct," AIAA Journal, Vol. 18, No. 12, Dec. 1980, pp. 1470-1476.
88. White, J. W., "A General Mapping Procedure for Variable Area Duct Acoustics," AIAA Paper 81-0094, Jan. 1981.
89. Walker, B. E., and Charwat, A. F., "Correlation of the Effects of Grazing Flow on the Impedance of Helmholtz Resonators," Journal of Acoustical Society of America, Vol. 72, No. 2, Aug. 1982, pp. 550-555.
90. Hersh, A. S., and Walker, B., "Effect of Grazing Flow on the Acoustic Impedance of Helmholtz Resonators Consisting of Single and Clustered Orifices," NASA CR 3177, Aug. 1979.
91. Koci, J. W., and Sarin, S. L., "An Experimental Study of the Acoustic Impedance of Helmholtz Resonator Arrays Under a Turbulent Boundary Layer," AIAA Paper 81-1998, Oct. 1981.
92. Rice, E. J., "A Model for the Acoustic Impedance of Linear Suppressor Materials Bonded on Perforated Plate," AIAA Paper 81-1999, Oct. 1981, (also NASA TM 82716).
93. Hersh, A. S., Walker, B., and Dong, S. B., "Analytical and Experimental Investigation of the Propagation and Attenuation of Sound in Extended Reaction Liners," AIAA Paper 81-2014, Oct. 1981.
94. Kuntz, H. L., "High-Intensity Sound in Air Saturated, Fibrous Bulk Porous Materials," Ph.D. Thesis, The University of Texas at Austin, Aug. 1982, (also NASA CR 167979).
95. Lambert, R. F., "Acoustical Structure of Highly Porous Open-Cell Elastic Foams," Journal of the Acoustical Society of America, Vol. 72, No. 3, Sept. 1982, pp. 879-887.

**ORIGINAL PAGE IS  
OF POOR QUALITY**